JOURNAL OF APPLIED ELECTROCHEMISTRY 11 (1981) 11–21

Behaviour of lead electrodes in sulphate electrolytes. I. Effect of electrode preparation on discriminant curve cyclic voltammograms

S. FLETCHER*, D. B. MATTHEWS

School of Physical Sciences, Flinders University of South Australia, Bedford Park, South Australia 5042, Australia

Received 6 May 1980

A new technique called discriminant curve cyclic voltammetry (DCCV) has been developed to study the cycling behaviour of battery plate materials. The method is used to investigate the effect of various electrode pretreatments on the cycling behaviour of pure lead in sulphate electrolytes. It is found that three distinctive patterns of response are observed depending upon the surface condition of the lead. The results are correlated with photographic evidence obtained by scanning electron microscopy.

1. Introduction

The electrochemical behaviour of lead electrodes in acidic sulphate electrolytes has been investigated for over one hundred years [1, 2]. Interest in this system was initially prompted, and continues still, because of its central role in the lead–acid battery. Several books and a number of reviews on this topic may be found in the literature [1–5]. The ultimate goal of research into the lead electrode/ sulphate electrolyte interface has been to improve the performance of the corresponding battery plate. In this paper we take up this theme, and in particular we report how certain pretreatment procedures influence the cycling behaviour of pure lead under laboratory conditions. The fundamental electrochemistry of many battery plates is poorly understood, and in this respect the lead–acid negative plate is no exception. Literature data are often conflicting (even the number of peaks in the voltammogram is controversial [6–14]) and vary from researcher to researcher by nearly two orders of magnitude. In the circumstances it is hardly surprising to find widespread disagreement concerning the mechanisms of the reactions involved.

The sources of the difficulties with the negative plate may be traced back to three fundamental causes. Firstly, different researchers have chosen different preparations and pretreatments for their electrodes [6–14]. It has been pointed out elsewhere how crucial this can be for solid electrodes [15] and obviously this makes comparison between the results of different workers rather difficult. Secondly, the experimental data are inherently nonlinear [16] and hence are very sensitive to interferences such as potentiostat noise, *iR* drop, etc. Thirdly, there has been until recently an absence of appropriate models for the electrocrystallization of thick films [17] and this has meant that the interpretation of data has been necessarily restricted.

Bearing in mind the above limitations, we compare in the present work the effects of different electrode pretreatments on subsequent experimental results, and we do this by a new technique which we call discriminant curve cyclic voltammetry (DCCV). In this technique a large number of cyclic voltammograms are recorded along the time axis (rather than the electrode–potential axis) and the time scale is compressed so that the discriminant curve created by many scans is easily seen. This technique has the advantage that small changes in the voltammograms are highlighted and, as we shall see, these changes are strongly influenced by the electrode pretreatment.

The effects of different electrode pretreatments were also investigated by scanning electron microscopy. Where possible, various structural features

---

* Present address: CSIRO Division of Mineral Chemistry, PO Box 124, Port Melbourne, Victoria 3207, Australia.

0021–891X/81/010011–11$03.10/0

are identified with changes in the DCCV response. Since the present work has the limited aim of investigating electrode pretreatment effects, no mechanistic analysis will be performed here. A full mechanistic analysis will however be the subject of a separate paper (Part 2 of this series).

2. Experimental

The constant potential source was a PAR 173 potentiostat. The voltage scan generator was a Wenking model VSG 72. Potentials were checked with a Hewlett-Packard 3465 A multimeter, calibrated against a Flinders University standard. The experimental apparatus was shielded to minimize noise, which was measured using a Tektronix type IL5 spectrum analyser. The strongest spurious signal was a 50 Hz (mains) noise whose amplitude was < 0.2 mV. All other noise signals were at least 30 dB down from the 50 Hz signal in the measurable range (10–1 MHz). Data were recorded on two recorders, a Houston Omnigraphic 2000 and a Hitachi QD 25 fast response recorder. The measured *iR* drop was approximately 1.2 Ω. The random potential step generator was designed and built at Flinders University.

Reference electrodes were either commercial pH-type saturated calomel electrodes or Hg/Hg_2SO_4 electrodes in the same solution as the working electrode. These latter reference electrodes were prepared according to the procedure recommended by Ives and Janz [18]. Lead electrodes were constructed from 99.999% lead sheet supplied by Koch-Light, and all chemicals used were Aristar grade.

Two cell designs were used in the present work. One was a rotating disc cell of conventional design, but including an adjustable luggin reference probe to minimize *iR* drop. The other was a fixed luggin two-compartment cell for vertically mounted electrodes. All solutions were prepared using water which had been triply distilled under nitrogen atmosphere. Cell solutions were deoxygenated using pure nitrogen. Experiments were performed at room temperature (~ 21° C). Before any experiments were begun, all electrodes were held at potentials negative to the Pb/$PbSO_4$ potential for two hours in order to reduce any oxidation products formed by aerial oxidation during the pretreatment procedures. The negative potential was not sufficiently large, however, to cause significant hydrogen evolution at the electrodes.

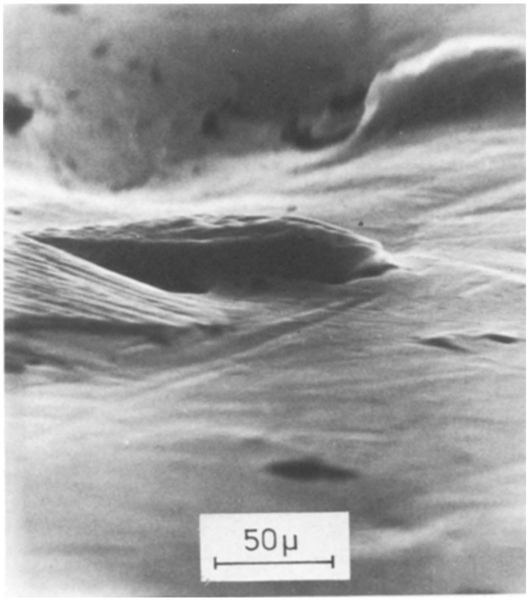

Fig. 1. Low-angle SEM photograph of a lead surface polished with commercial polishing cloth.

3. Electrode preparation

Three different polishing procedures were investigated which were characterized by the polishing materials employed. Polishing materials tried were (a) cellulose fibre, (b) alumina followed by commercial polishing cloth ('Selvyt') and (c) various grades of emery paper. The cellulose-fibre polishing procedure (using alcohol or acetone as a wetting agent) was found by scanning electron microscopy (SEM) to produce a featureless surface down to 100x magnification; microscopic irregularities were sheared from the surface in this case. Polishing with Selvyt, again using alcohol or acetone, tended to 'smear' the surface producing undulations in a more or less featureless terrain (Fig. 1). Carbide paper, both wet and dry, invariably produced a surface both sheared and smeared and which contained massive numbers of irregularities (Fig. 2).

Aside from the three mechanical preparation procedures described above, three further treatments were (a) immersion of the electrode in

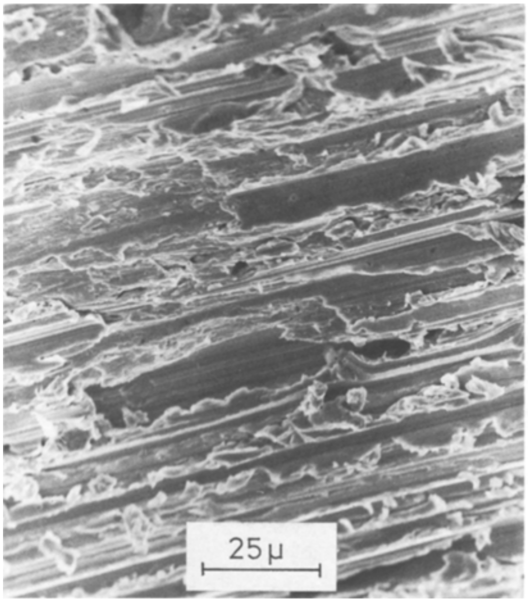

Fig. 2. 45° angle of incidence SEM photograph of a lead surface polished with carbide paper.

triply-distilled water in an ultrasonic bath for twenty minutes, (b) evolving hydrogen from the electrode surface prior to making any measurements and (c) cycling the electrode ten times through the Pb/PbSO$_4$ active–passive transition at 200 mV s^{-1}. Treatments (a) and (b) both produced similar physical effects on the morphology of the resulting surfaces: irregular pitting of all surfaces was observed. A typical SEM picture of pitting of a carbide-prepared surface, after immersion in the ultrasonic bath, is shown in Fig. 3. A picture of a cellulose-fibre polished electrode after 20 minutes in hydrogen evolution is shown in Fig. 4. As we shall see later, the presence of both roughness and pits strongly influences experimental results in this system. The effect of the cycling treatment (c) applied to 'carbide-polished' and 'cellulose-fibre polished' electrodes was to produce massive surface rearrangement in both instances. In the case of fibre-polished electrodes, cracks appeared in the surface and residual crystalline nuclei of PbSO$_4$ were trapped in the surface layer of lead (Fig. 5). In the case of carbide-polished (microscopically rough) electrodes, the surface became covered with microscopic dendrites of redeposited lead (Fig. 6).

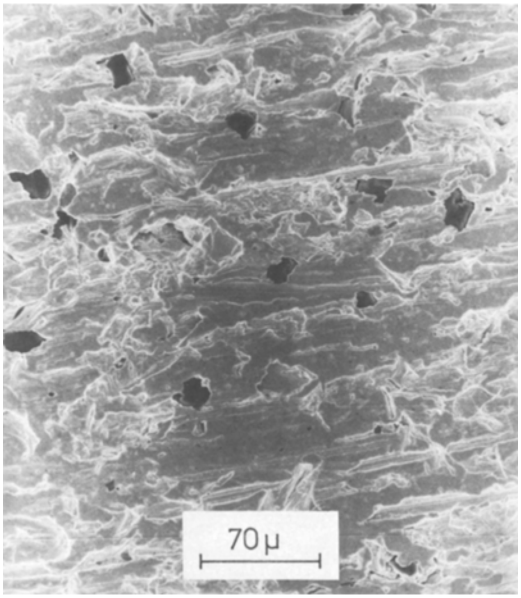

Fig. 3. Vertical shot of a carbide-paper polished electrode after 20 minutes ultrasonic cleaning. Note extensive pitting.

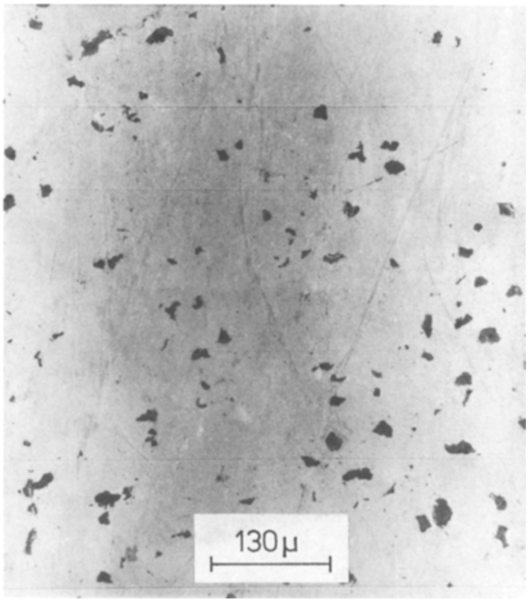

Fig. 4. Vertical shot of a cellulose-fibre polished electrode after 20 minutes in H_2 evolution (at − 1800 mV versus SCE in 0.5 M H_2SO_4). Note extensive pitting.

Further complications were introduced by cycling electrodes through the Pb/PbSO$_4$ region several hundred times. This process always resulted in the irreversible deposition of a thick deposit of 'insoluble' PbSO$_4$. Leaving such a surface on open circuit for three days failed to remove this layer,

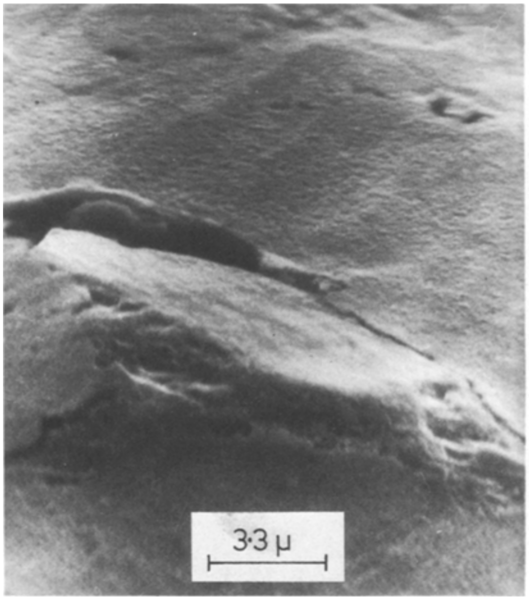

Fig. 5. 60° angle of incidence SEM photograph of a cellulose-fibre polished electrode, cycled ten times through the Pb → $PbSO_4$ transition. Note residual crystal of $PbSO_4$ 'trapped' by redeposited lead.

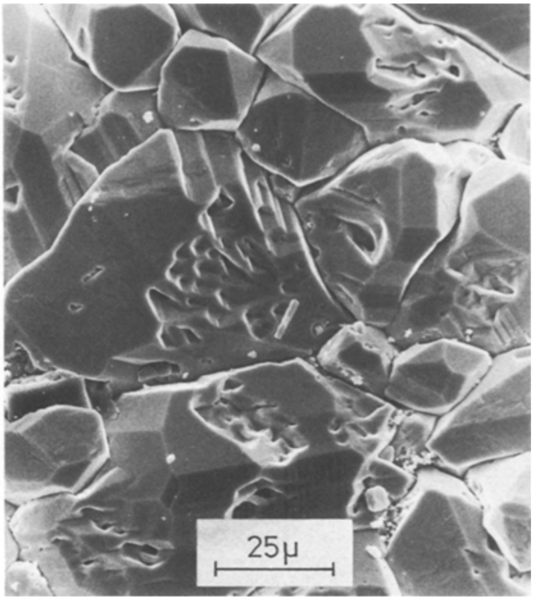

Fig. 7. Vertical shot of electrode surface polished with commercial polishing cloth, after several hundred cycles through the Pb → $PbSO_4$ transition. Note residual 'hard' sulphate still remaining after three days on open circuit.

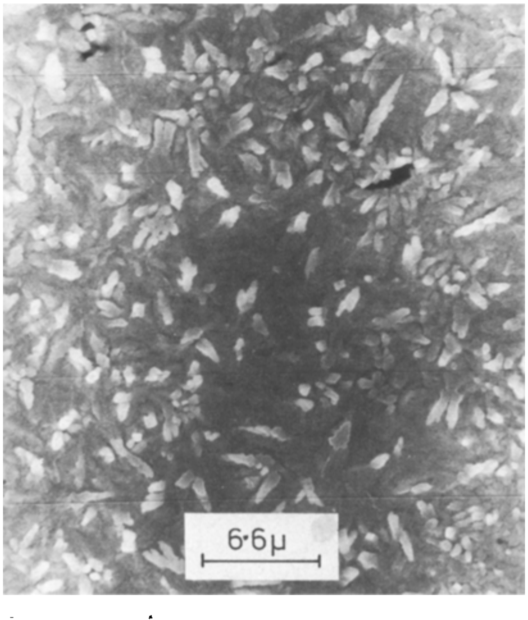

Fig. 6. Vertical shot of hydrogen-evolution roughened, carbide-paper polished electrode after ten cycles through the Pb → $PbSO_4$ transition. Note dendritic crystals of lead redeposited on surface.

although some etch pits could be seen in the crystals (Fig. 7). The deposit could be removed, however, by holding the electrode at negative potentials corresponding to copious hydrogen evolution (bubbles visible to the naked eye). Under these circumstances the layer could be entirely removed in ten minutes. At rather less negative potentials (200 mV cathodic to the open circuit potential) it required almost two hours to fully reduce the $PbSO_4$ back to lead.

It is apparent from Figs. 1–7 that many different types of surface could be created on lead electrodes in sulphate electrolytes. The problem, however, was to decide which of these surfaces could be generated reproducibly so that valid kinetic conclusions could be drawn from any subsequent electrochemistry. It was also important to decide which surface most closely resembled the operating surface of the lead battery plate. To this end we developed the technique of discriminant curve cyclic voltammetry (DCCV) in order to understand the cycling behaviour of variously-prepared electrodes. But before describing the experimental results, we briefly summarize some of the mathematical features of DCCV. In what follows we shall quote a number of standard mathematical definitions; they are not, of course, original but are reproduced here for the convenience of the reader.

4. Definition of the discriminant curve

Before defining the discriminant curve, we first introduce the idea of an envelope. If we have a family of curves (such as a series of voltammograms displayed along the time axis) then the new curve which is revealed to be tangential at each of its points to some individual curve (voltammogram) of the family is called the envelope of the given family. In general we can write the equation of a family of voltammograms in the form

$$f(X, Y, \alpha_1, \alpha_2, \alpha_3 \ldots \alpha_n) = 0 \qquad (1)$$

where X and Y are co-ordinates of points, and the α_i are parameters (auxiliary variables) which control the translation of the curve over the x–y plane. In the present work we have

$$X = i\,(\mathrm{mA\,cm^{-2}})$$

$$Y = t\,(\mathrm{s})$$

$$\alpha_1 = \text{cycle number (dimensionless)}$$

$$\alpha_2, \alpha_3 \ldots \alpha_n = \text{constants}$$

but of course many other X, Y, and α_i are possible. It follows that, in general, the solution of Equation 1 requires $n - 1$ unique relations between the parameters

$$\begin{aligned} f_1\,(\alpha_1, \alpha_2, \ldots \alpha_n) &= 0 \\ f_2\,(\alpha_1, \alpha_2, \ldots \alpha_n) &= 0 \\ &\vdots \\ f_{n-1}(\alpha_1, \alpha_2, \ldots \alpha_n) &= 0. \end{aligned} \qquad (2)$$

Given these relations it can easily be shown that the envelope curve always satisfies the solution obtained by inserting Equations 2 into Equation 1. For instance, if Equations 1 and 2 are polynomial in the α_i, then the envelope satisfies the equation obtained by adjoining

$$\begin{vmatrix} f_{\alpha_1} & f_{\alpha_2} & \cdots & f_{\alpha_n} \\ (f_1)_{\alpha_1} & (f_1)_{\alpha_2} & \cdots & (f_1)_{\alpha_n} \\ (f_2)_{\alpha_1} & (f_2)_{\alpha_2} & \cdots & (f_2)_{\alpha_n} \\ \vdots & & & \\ (f_{n-1})_{\alpha_1} & (f_{n-1})_{\alpha_2} & \cdots & (f_{n-1})_{\alpha_n} \end{vmatrix} = 0 \qquad (3)$$

to Equations 1 and 2 and eliminating the parameters α_i.

Since the envelope of the family of voltammograms satisfies the equation obtained by eliminating parameters from Equations 1 and 2 it is reasonable to ask if the envelope, as defined, uniquely exhausts *all* points whose co-ordinates satisfy the derived solution. The answer is no; the curve described by the equation is actually called the discriminant curve of the family of voltammograms and while the discriminant curve includes the envelope, it may also contain points (or regions) which are not considered in our definition of an envelope. These points (or regions) are caused by the presence of singular points existing in the original family of voltammograms. Such singular points could be, for example, points of self-intersection, cusps, etc. (see Fig. 8). And it turns out that the loci of all singular points also contribute to the discriminant curve. Fortunately for us, it can be shown that the envelope and the loci of all singular points exhaust all regions of the discriminant curve with probability one [19]. Thus we can define the discriminant curve as that curve which consists of both the envelope and the loci of all singular points of the curves of the family.

Given the above facts it is clear that cyclic voltammetry, producing as it does a family of curves, can be made to trace out a discriminant curve by variation of one parameter. In the present work we use the cycle number as the discrete variable and trace out discriminant curves as a function of this variable. This procedure is analagous to investigating the charge–discharge behaviour of a battery plate directly. Even though we are not able to solve the mathematical model in the particular case under consideration (since we do not know the functional form of Equation 1), the qualitative analysis of discriminant curves from cyclic voltammetry nevertheless reveals a good deal about the cycle life of the lead electrode in sulphate electrolytes. In particular it allows us to monitor variations in cycle life, maximum current etc., in a simple and elegant way.

The practical realization of a discriminant curve is also illustrated in Fig. 8. First, a cyclic voltammogram is displayed on the time axis rather than the electrode potential axis (note that a pseudo-peak may appear where the scan turns

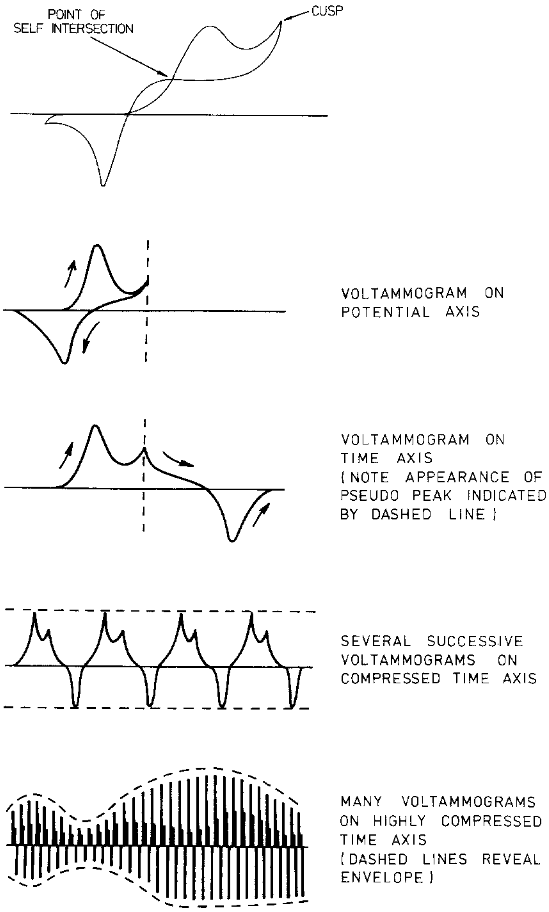

Fig. 8. Some singular points which occur in a cyclic voltammogram. Most voltammograms will have a small finite number of singular points, and in particular a cusp at each end. (If a voltammogram has no singular points it is said to be smooth.) It follows that any voltammogram is divided into smooth arcs by its singular points. Hence the discriminant curve of any family of voltammograms will contain envelopes from the smooth regions and also the loci of all singular points.

around, due to the cusp in the original voltammogram). Then the time axis is more and more compressed until the individual voltammograms appear only as thin vertical lines (bottom illustration). At this stage the discriminant curve becomes visible and may be traced through the figure. At the top and bottom of the final picture, sections of the discriminant curve are outlined by a dashed curve. This dashed curve is the *envelope* of the family of displayed voltammograms. Inside the family of voltammograms a third section of the discriminant curve is just visible, due to the psuedo-peak arising from the original cusp. For fairly obvious reasons, we call the technique which leads to the full display *discriminant curve cyclic voltammetry*. It differs from ordinary cyclic voltammetry only in the way the data are displayed, our particular choice of display being selected for its ability to highlight slowly evolving changes in the individual voltammograms. The discriminant curve is a convenient measure of these slowly evolving changes.

5. Results

In the DCCV measurements the electrode potential was scanned repetitively through the $Pb/PbSO_4$ region after various pretreatment procedures. Several different electrolytes were used and differences in i_p as a function of cycle number were then followed as the upper envelope of the curves. A typical result is shown in Fig. 9a which shows seven successive sets of DCCV responses with hydrogen evolution in between, all recorded on the same electrode. By appropriate compression of the time scale the discriminant curves can be viewed directly, the upper (anodic) envelope being of immediate interest. In this illustration the first set of cycles shows what turned out to be the very typical falling response of a cellulose-fibre polished ('smooth') electrode in which the peak height (i_p) for the $Pb \rightarrow PbSO_4$ reaction rapidly falls to a constant value. We call this 'type I' behaviour. If such an electrode is then treated by evolving hydrogen for five minutes it is found that similar falling behaviour is observed, except that the absolute value of i_p approximately doubles in magnitude. When this procedure is repeated a number of times the shape of the DCCV response changes so that i_p, after initially falling, gradually begins to rise. This falling–rising behaviour of i_p we classify as 'type II'. If the hydrogen evolution treatment is repeated 15 or 20 times then eventually a limiting response is obtained in which i_p does not have a minimum at all, but rather has a constant, steady value. We call this limiting behaviour (which is highly reproducible from experiment to experiment) 'type III'. An example of type III behaviour is illustrated in Fig. 9b.

It turned out that type I behaviour could only be observed in the present work with cellulose-fibre polished electrodes. On the other hand reproducible type III behaviour could be observed independent of all pretreatment procedures tried in the present work, provided sufficient hydrogen

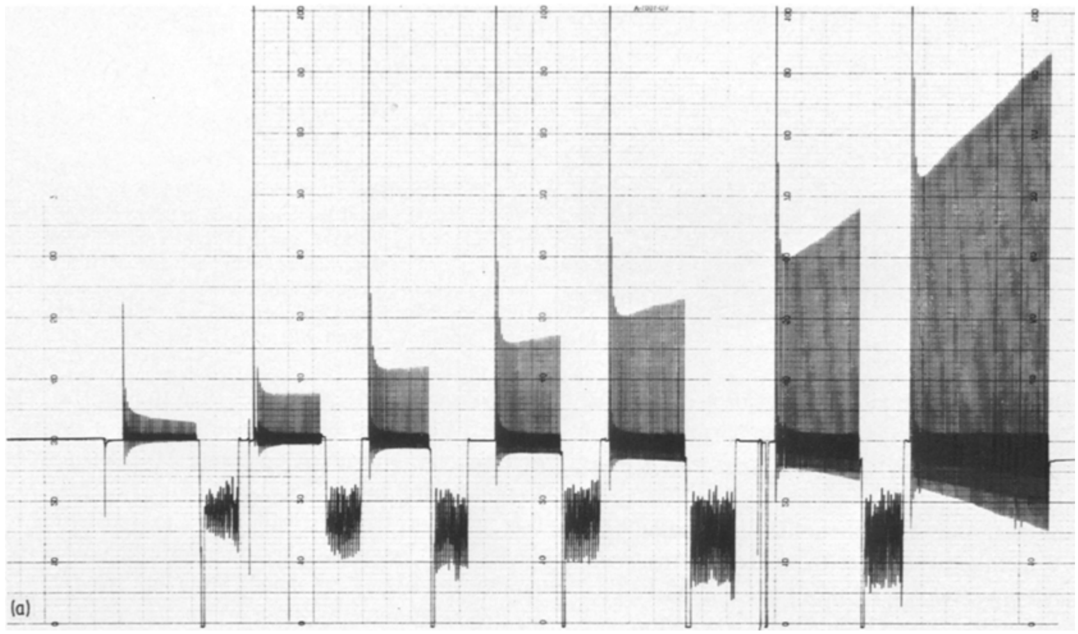

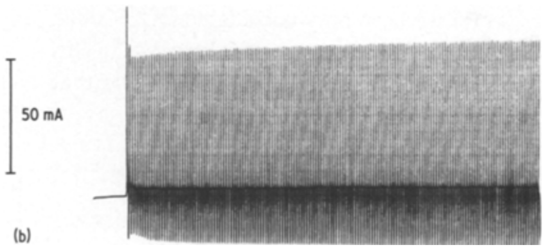

Fig. 9. (a) Effect on discriminant curve cyclic voltammograms of successive excursions into hydrogen evolution. Lead electrode initially highly polished with cellulose fibre. Electrolyte 0.5 M H_2SO_4, scans from -1000 mV to 0 mV versus SCE at 200 mV s^{-1}. Vertical axis 50 mA full scale. Electrode area 0.5 cm^2. Current densities for H_2 evolution were divided by a factor of 10 to bring them on scale. Hydrogen was evolved for three-minute bursts at -1800 mV. (b) Discriminant curve cyclic voltammogram of type III electrode in 0.5 M H_2SO_4. Scans from -1000 mV to 0 mV versus SCE at 200 mV s^{-1}; vertical axis 50 mA/division; electrode area 0.5 cm^2.

evolution was carried out prior to any measurements being made. The type II behaviour was observed with all other preparation methods, but with varied results. For example, the minimum in i_p after 6–8 cycles varied in magnitude by a factor of ten depending on the pretreatment method employed. The difference between the smallest recorded i_p and the largest recorded i_p was about two orders of magnitude overall, in keeping with the disparate values of i_p reported in the literature [6–14]. In general we found that smooth electrodes without pits gave low values of i_p whereas rough electrodes with pits gave high values of i_p.

The rather interesting results shown in Fig. 9 are not confined to pure 0.5 M sulphuric acid electrolytes. Fig. 10 shows the effect of just five seconds of hydrogen evolution on the DCCV response of a cellulose-fibre polished lead electrode in 0.5 M $(NH_4)_2SO_4$ electrolyte (adjusted to pH 4.0 with H_2SO_4). There is an immediate increase in i_p by a factor of approximately five. Note that this electrolyte yields a new type of DCCV response too, in which i_p not only has a local minimum after 5–6 cycles but also a local maximum after 17–18 cycles. The effect of electrolyte on DCCV response is clearly complex in this case.

The DCCV method can also be used to investigate the extended 'cycle life' of an electrode. As an illustration of this we show in Fig. 11 the behaviour of a type II electrode in 0.5 M H_2SO_4 over more than 6000 cycles. For convenience the DCCV upper envelope is plotted on logarithmic scales. The result shows a maximum in i_p after 800 cycles with a half-peak width (ΔC) of about 1000 cycles. Logarithmic DCCV plots of this type may prove useful from the point of view of

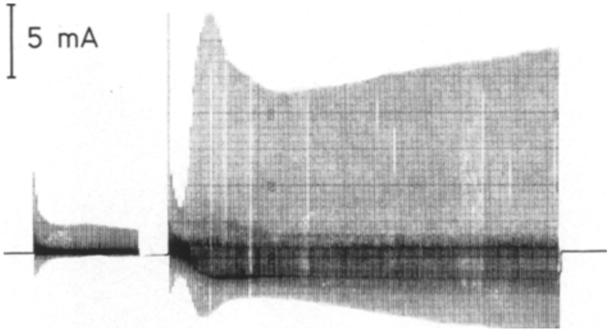

Fig. 10. DCCV of cellulose-fibre polished lead electrode in 0.5 M $(NH_4)_2SO_4$, pH 4.04. Vertical scale 5 mA/division; electrode area 0.5 cm². Effect of 5 s hydrogen evolution at – 2.0 V versus SCE. Scans from – 1000 mV to 0 mV versus SCE at 200 mV s^{-1}.

battery development since in that type of work it is often desirable to maximize the performance of individual battery plates (i.e., maximize i_p, q and ΔC).

Another interesting phenomenon revealed by DCCV was the persistence of surface pretreatment effects even after several thousand cycles of electrode potential through the Pb/PbSO$_4$ region. Fig. 12 shows the different DCCV responses of type I and type III electrodes over several thousand cycles in 0.5 M $(NH_4)_2SO_4$ electrolyte (pH 4.0). Although the type I electrodes increase their i_p after ~80 cycles, the overall DCCV response is typically 20 x lower than that of the type III electrodes over the whole range of cycles investigated. This persistence suggests that in order to understand the cycling behaviour of i_p (and q) it is sufficient to investigate only the first 100 cycles or so, which implies the possibility of rapidly screening many electrolyte additives, electrode alloying materials etc. in order to maximize battery plate performance. We shall take up this point in greater detail in a future paper.

So far we have only considered DCCV data recorded using a scan rate of 200 mV s^{-1}. This scan rate drives the electrochemical reations at

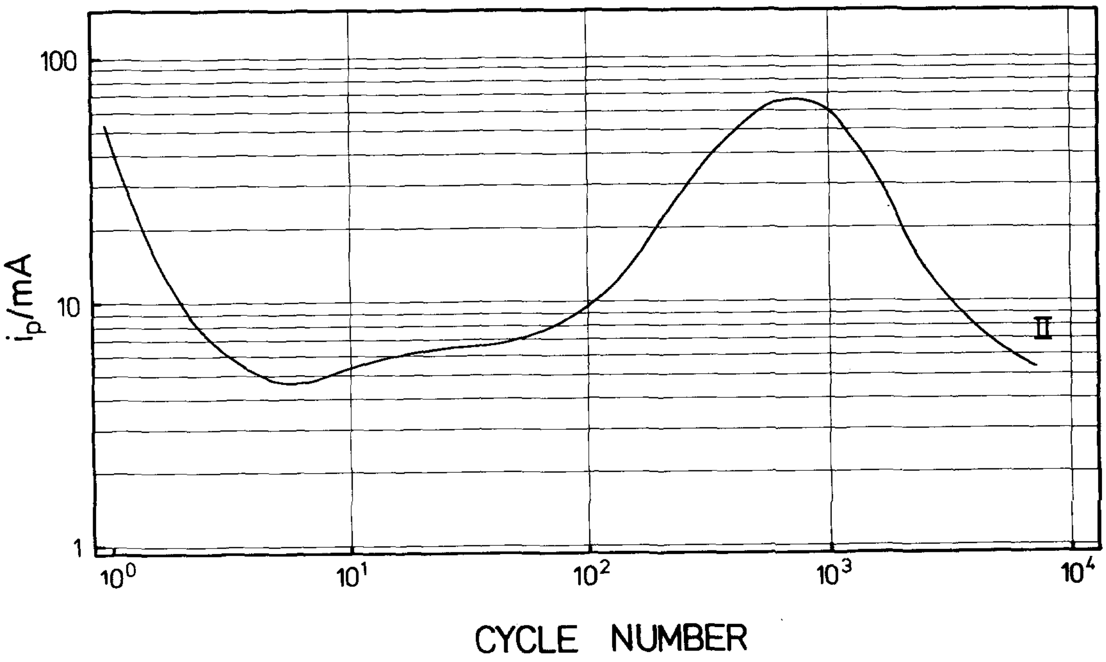

Fig. 11. DCCV envelope for a type II lead electrode in 0.5 M H_2SO_4. Scans from – 1000 mV to 0 mV versus SCE at 200 mV s^{-1}. Electrode area 0.5 cm².

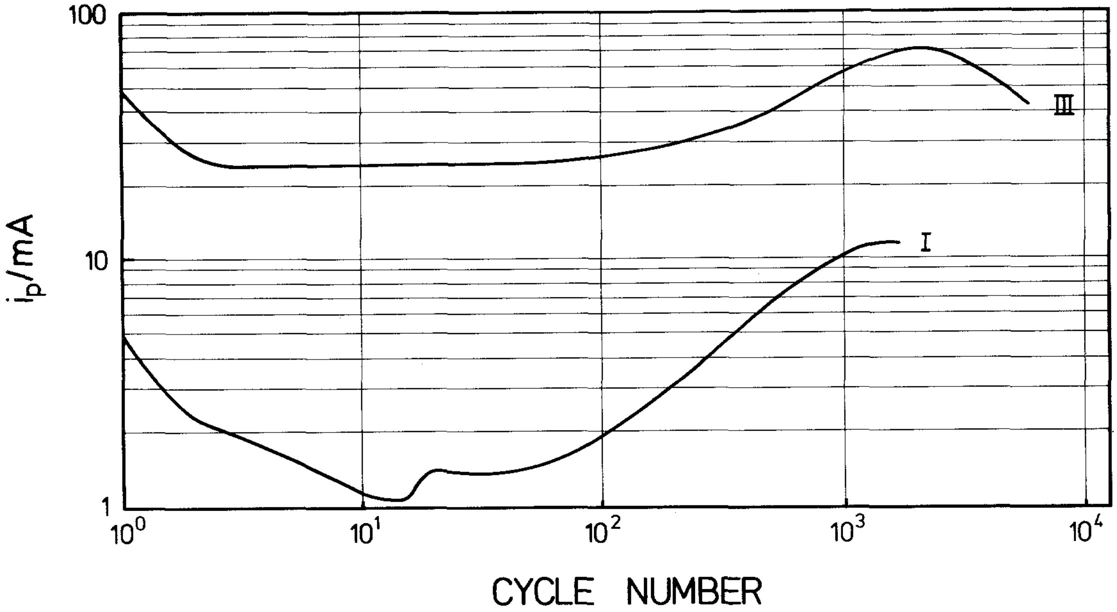

Fig. 12. DCCV envelopes for type I (bottom) and type II (top) lead electrodes in 0.5 M $(NH_4)_2SO_4$ solution, pH 4.04. Scans from — 100 mV to 0 mV versus SCE at 200 mV s^{-1}. Electrode area 0.5 cm^2.

the lead electrode much faster than is actually encountered in working batteries, such as in electric vehicle applications for example. But similar data are obtained using scan rates 1000 x slower, although this is rather tedious to collect because of the lengthy time scales involved. Fig. 13 shows type II and type III behaviour recorded at 0.2 mV s^{-1} in pure 0.5 M H_2SO_4. On this time scale the type III behaviour was remarkably constant, whereas type I behaviour could not be observed at all. (Electrodes which were cellulose-fibre polished invariably produced type II behaviour on this time scale rather than type I behaviour.)

Because the DCCV data were obtained using a

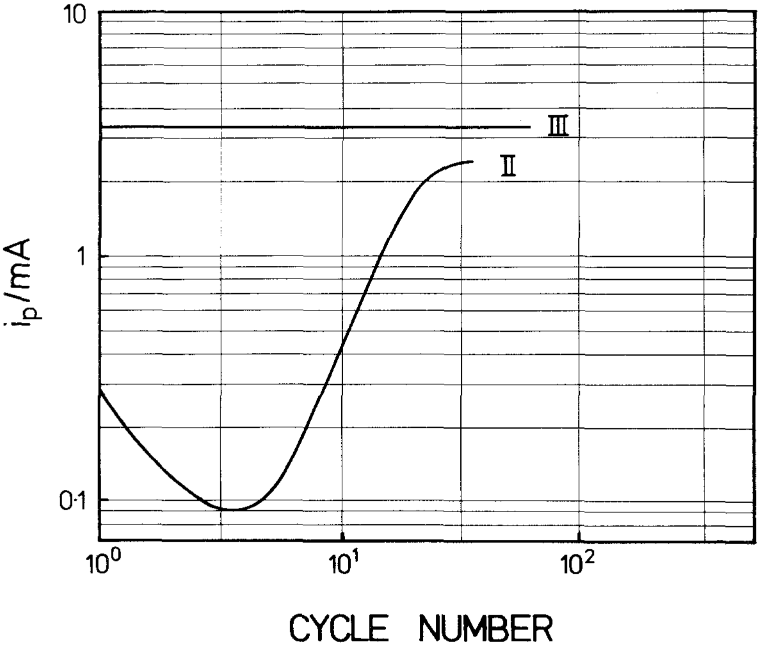

Fig. 13. DCCV envelopes for 'fibre-smooth' (bottom) and hydrogen roughened, type III electrodes (top) in 0.5 M H_2SO_4. Scans from — 630 to — 430 mV versus SCE at 0.2 mV s^{-1}. Electrode area 0.5 cm^2.

periodic triangular potential waveform, we also checked what influence the periodicity had on the experimental results. We achieved this by using a potential step of the same amplitude as the triangular potential waveform, but triggered randomly in time with a random pulse generator. The pulses were distributed as a Poisson point process with $\mu = 2.5$ s. The same general behaviour of i_p as a function of cycle number was observed, depending on pretreatment, except that the i_p envelope was 'noisy'. Electrodes of types I, II and III could readily be distinguished as in the DCCV cases.

6. Conclusion

In the past the behaviour of lead electrodes in sulphate electrolytes has been known to be irreproducible in two distinct ways [6–14]. Firstly, different electrode preparation procedures used by different workers led to different values of kinetic parameters (such as i_p in linear potential scan experiments). Secondly, internally consistent data were difficult to obtain because individual kinetic measurements within one experiment caused uncontrolled variations in all subsequent measurements. Thus, the very act of recording experimental data caused time-varying changes in the surface condition of the electrodes. In this paper we have investigated both types of irreproducibility using scanning electron microscopy (SEM) and discriminant curve cyclic voltammetry (DCCV).

Despite the large differences in pretreatment procedures used in the present work, and the massive morphological differences in electrode surfaces revealed by SEM, it was nevertheless found by DCCV that lead electrodes in sulphuric acid electrolytes could be classified into three basic categories. In the category we call type I the electrodes exhibited a falling i_p for the $Pb \rightarrow PbSO_4$ transition as a function of cycle number. This falling behaviour persisted for about 100 cycles and was found to correlate with smooth surfaces. In the type II category the value of i_p showed a minimum after about 6–8 cycles and thereafter i_p continued to rise for several hundred cycles. Type II electrodes were created by many different polishing procedures and recorded values of i_p for this class of electrodes differed by almost two orders of magnitude. Type II behaviour was almost certainly connected with microscopic surface defects, of many different varieties, created as a consequence of the different pretreatment procedures. Type III behaviour, in which i_p remained constant between the third and eightieth cycles, was found after extensive *in situ* hydrogen evolution coupled alternately with bursts of cycling through the $Pb/PbSO_4$ transition. Type III electrodes were characterized by the presence of widespread pitting caused by the hydrogen evolution reaction.

Because pitting caused by the ultrasonification of electrodes resulted in type II electrodes rather than III, it cannot be claimed that the presence of pits uniquely defines a type III electrode. Rather, pits are a necessary, but not sufficient, criterion that a given electrode belongs to the type III category. Type III electrodes could be reproducibly made from experiment to experiment, and furthermore they could be regenerated inside the cell by the simple expedient of evolving hydrogen. It follows that type III electrodes are the most suitable for recording reproducible kinetic data on the $Pb \rightarrow PbSO_4$ transition.

Acknowledgements

The authors would like to thank S. P. S. Badwal for a number of conversations, J. Pezy for constructing the random pulse generator and R. W. Garrad for operating the scanning electron microscope. The authors would also like to thank the Flinders University Plasma Physics group for the loan of the noise spectrum analyser, and the Flinders University Electric Vehicle Project for the loan of the fast-response pen recorder. One of us (S.F.) would also like to thank the Department of Transport of the Government of South Australia for a fellowship.

References

[1] H. Bode, in 'Lead–Acid Batteries', J. Wiley and Sons, New York (1977).
[2] G. W. Vinal, in 'Storage Batteries', 4th edn, J. Wiley and Sons, New York (1955).
[3] D. V. Kordesch, in 'Batteries', Vol. 2, Marcel Dekker, New York (1977).
[4] J. Burbank, A. C. Simon and E. Willihnganz, in 'Advances in Electrochemistry and Electrochemical Engineering', Vol 8 (edited by P. Delahay and L. W. Tobias) (1971) p. 157.

[5] T. F. Sharpe, in 'The Electrochemistry of the Elements' (edited by A. J. Bard) (1970).
[6] A. N. Fleming and J. A. Harrison, *Electrochim. Acta* 21 (1976) 905 (and references therein).
[7] N. A. Hampson and J. B. Lakeman, *J. Power Sources* 4 (1979) 21 (and references therein).
[8] P. Ruetschi, *J. Electrochem. Soc.* **120** (1973) 331.
[9] D. Pavlov and R. Popova, *Electrochim. Acta* 15 (1970) 1483 (and references therein).
[10] T. G. Chang, M. M. Wright and E. M. L. Valeriote, in 'Power Sources 6' (edited by D. H. Collins) Academic Press, New York (1977).
[11] H. S. Panesar in "Power Sources 3' (edited by D. H. Collins) Oriel Press, Newcastle (1971).
[12] J. P. Carr, N. A. Hampson and R. Taylor, *J. Electroanal. Chem.* **33** (1971) 109.
[13] T. F. Sharpe, *J. Electrochem. Soc.* **122** (1975) 845.
[14] M. P. J. Brennan, B. N. Stirrup and N. A. Hampson, *J. Appl. Electrochem.* 4 (1974) 49.
[15] M. Sluyters-Rehbach and J. H. Sluyters in 'Electroanalytical Chemistry', Vol. 4 (edited by A. J. Bard) Marcel Dekker, New York (1970) p. 64.
[16] M. Fleischmann, in 'Introduction to the Faraday Discussions' (no. 12), University of Southampton, England (1977).
[17] S. Fletcher and D. Matthews, *J. Appl. Electrochem.* 11 (1981) 1.
[18] D. J. G. Ives and G. J. Janz 'Reference Electrodes' Academic Press, New York (1961) p. 335.
[19] V. G. Boltyanskii, 'Envelopes', Pergamon Press, Oxford (1964).

Note. This reference list is not intended to be exhaustive, but merely indicates major trends during the last decade or so.